Computer Simulation of Feedback Induced Noise in Semiconductor Lasers Operating with Self-Sustained Pulsation

IEICE TRANS. ELECTRON., VOL. E81–C, NO. 5 MAY 1998

PAPER

Computer Simulation of Feedback Induced Noise in Semiconductor Lasers Operating with Self-Sustained Pulsation

Minoru YAMADA[†a)], *Member*

SUMMARY Theoretical calculations of the pulsing operation and the intensity noise under the optical feedback are demonstrated for operation of the self-sustained pulsation lasers. Two alternative models for the optical feedback effect, namely the time delayed injection model and the external cavity model, are applied in a combined manner to analyze the phenomena. The calculation starts by supposing the geometrical structure of the laser and the material parameters, and are ended by evaluating the noise. Characteristics of the feedback induced noise for variations of the operating parameters, such as the injection current, the feedback distance and the feedback ratio, are examined. A comparison to experimental data is also given to ensure accuracy of the calculation.

key words: *semiconductor laser, feedback induced noise, self-sustained pulsation, self-pulsing lasers, saturable absorption, mode competition phenomena, optical disk system*

1. Introduction

Semiconductor lasers reveal the so called feedback induced noise due to re-injection of the output light reflected at the surface of a connecting optical device such as the optical disk or the optical fiber. Superposition of a high-frequency current on the injection laser and the effect of the self-sustained pulsation have been found in experiments to be effective to reduce the feedback induced noise [1], [2].

The generating mechanism of the feedback induced noise has been explained in terms of the mode competition phenomena among the lasing modes of the laser cavity itself and the external cavity formed by the space between the laser facet and the reflecting point [3]–[6]. Mechanisms of the noise reduction by the superposition of a high-frequency and by the self-sustained pulsation have been also well explained as an effect of changing the operating state in the mode competition phenomena [7]–[9].

Since the application markets of the semiconductor lasers have been spread widely such as the magnet-optical (MO) disk system or the digital video disk (DVD) system, more profitable lasers with a wider range of output power and lower noise are required. Generation of the self-sustained pulsation was theoretically analyzed to be an effect caused by the saturable absorbing regions [10], resulting in experimental proposals of several improved structures [11]–[14].

This paper demonstrates computer simulations of the pulsation operation and the characteristics of the feedback induced noise in the self-sustained pulsation lasers. The calculation starts by supposing the structural parameters of the laser such as the material contamination and the geometrical size of each layer.

There are two alternative treatments to take into account effect of the optical feedback on variations of the photon number and the carrier density. One is to count time delay of the feedback to the lasing mode on optical propagation from the output [15]–[22]. The other is to count buildup of the external cavity modes formed by a space between the laser facet and the reflecting point [5], [6], [15]. The latter treatment seems better to analyze the feedback induced noise because the statistical behavior of the fluctuations on both the photon number and the carrier density are well formulated. However, this treatment has a difficulty on tracing exactly the external cavity modes during the pulsation because resonant conditions of the modes timely change with variation of the electron density in the laser through variation of the refractive index.

We apply those two treatments occasionally in this paper. The pulsing operation under the optical feedback is analyzed in Sect. 2 with the former treatment of the time delayed injection model by performing numerical integration for time variation. The feedback induced noise resulting from the mode competition phenomena is evaluated in Sect. 3 basing on the latter treatment. The calculation is equated with several timely averaged values consist of the photon number and the electron density which are pre-evaluated through determination of the pulsing operation in Sect. 2. Conclusions and remarks are given in Sect. 4.

Examples treated by numerical calculations are included in both Sects. 2 and 3. Model of the calculation is a laser for the compact disk (CD) system or the video disk (VD) system, where the current blocking region works as the saturable absorbing region and the pulsing operation is limited up to several mW. Experimentally measured data of the feedback noise are also referred to ensure accuracy of the calculation.

Manuscript received December 3, 1997.

[†]The author is with the Faculty of Engineering, Kanazawa University, Kanazawa-shi, 920–8667 Japan.

a) E-mail: myamada@t.kanazawa-u.ac.jp

2. Pulsing Operation under Optical Feedback

2.1 Basic Equations

Output light from a laser is reflected by a surface of connected optical device and re-injected into the laser as illustrated in Fig. 1, where R_b and R_f are the power reflectivities of the back and the front facets, respectively, L is length of the laser, ℓ is the feedback distance, Γ ($0 \leqq \Gamma \leqq 1$) is the feedback ratio, η ($0 \leqq \eta \leqq 1$) is the coupling efficiency to the lasing mode in the laser.

Electric field E in the laser is represented with injected component E_{inj} as

$$E = \sum_p \left[\sqrt{\frac{\hbar\omega_p}{2\varepsilon_o n_r^2} S_p(t)}\ \Phi_p(\mathbf{r})\ e^{j\varphi_p(t)+j\omega_p t} + c.c. \right] + E_{inj} \tag{1}$$

where, n_r is an effective refractive index and p represents number of a mode in the laser itself which is called internal cavity mode in this paper. S_p is photon number and $\Phi_p(\mathbf{r})$ is a spatial field distribution function normalized in the laser. ω_p is the optical angular frequency when the laser is assumed in the continuos wave (CW) operation neither with the self-sustained pulsation nor with the optical feedback. $\varphi_p(t)$ is a phase term added to $\omega_p t$ to indicate the real optical phase. The optical angular frequency at a time t is given by $\omega_p + d\varphi_p(t)/dt$. The injected field E_{inj} must be represented with the same mode components but with a different angular frequency such as $\omega_p + d\varphi_p(t-\tau)/dt$ generated at $t-\tau$, where

$$\tau = 2\ell/c \tag{2}$$

is a delay time due to one round trip to the reflecting point located at the distance ℓ.

By substituting Eq. (1) into the classical electromagnetic field equation and the density matrix equation of the electron motion, the following dynamic equations of the photon number S_p, the optical phase φ_p and the carrier density n_i are obtained basing on a similar treatment used in deriving the rate equations in Ref. [24]. The nonlinear gain due to the internal cavity modes and the linear polarization caused by the re-injected light are included. By counting the feedback up to the second time round trip and neglecting terms with $d\sqrt{S_p(t-\tau)}/dt$ and $d\sqrt{S_p(t-2\tau)}/dt$, we get

$$\frac{dS_p}{dt} = \left[\sum_i A_{pi} - BS_p - \sum_{q \neq p} D_{pq} S_q - G_{th} \right] S_p + \sum_i C_{pi} + \mathrm{Re}\left\{ \sum_i [A_{pi} + j\alpha a_i \xi_i (n_i - \overline{n_i})] \sqrt{S_p(t)} \times \left[U_p^{(1)} \sqrt{S_p(t-\tau)} + U_p^{(2)} \sqrt{S_p(t-2\tau)} \right] \right\} \tag{3}$$

$$\frac{d\varphi_p}{dt} = \frac{\alpha}{2} \sum_i a_i \xi_i (n_i - \overline{n_i}) + \frac{1}{2} \mathrm{Im} \left\{ \sum_i [A_{pi} + j\alpha a_i \xi_i (n_i - \overline{n_i})] \left[U_p^{(1)} \sqrt{\frac{S_p(t-\tau)}{S_p(t)}} + U_p^{(2)} \sqrt{\frac{S_p(t-2\tau)}{S_p(t)}} \right] \right\} \tag{4}$$

$$\frac{dn_i}{dt} = -\frac{1}{V_i} \sum_p \left(A_{pi} \left| \sqrt{S_p(t)} + U_p^{(1)} \sqrt{S_p(t-\tau)} + U_p^{(2)} \sqrt{S_p(t-2\tau)} \right|^2 \right) - \frac{n_i}{\tau_{si}} + \sum_{j \neq i} \left(-\frac{n_i}{T_{ij}} + \frac{n_j V_j}{T_{ji} V_i} + \frac{I_{ji} - I_{ij}}{eV_i} \right) \tag{5}$$

The parameters included in the above simultaneous dynamic equations are defined and discussed in the followings:

The suffices i and j are numbers assigned to regions in the crosssectional structure of the laser shown Fig. 2.

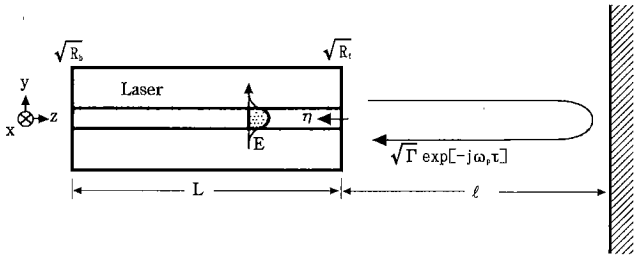

Fig. 1 Optical feedback to a laser. Length of the laser is L and the feedback distance is ℓ. The feedback ratio is Γ and the optical phase delay is $\omega_p\tau$. The coupling efficiency in the laser is η.

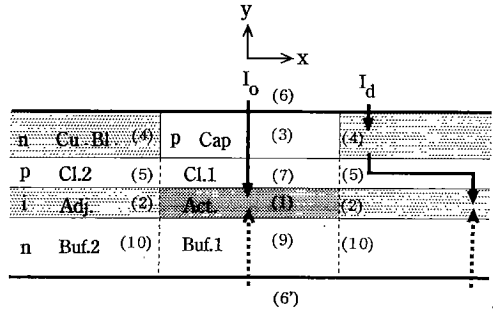

Fig. 2 Crosssectional view of the self-sustained pulsation laser. Act. is the active region, Adj. is the adjoining region, Cu.Bl. is the current blocking region and Cap is the cap region. All regions are also numbered. I_o is the principal injection current into the Act. region, while I_d is the diffusion current caused by the optical absorption in Cu.Bl. region.

A_{pi} is the linear gain coefficient of a mode p in region i,

$$A_{pi} = a_i \xi_i [n_i - n_{gi} - b(\omega_p - \omega_o)^2] \tag{6}$$

given with the slope coefficient a_i, the field confinement factor ξ_i defined by

$$\xi_i = \int_{V_i} |\Phi_p(\mathbf{r})|^2 d^3\mathbf{r} \Big/ \int_{laser} |\Phi_p(\mathbf{r})|^2 d^3\mathbf{r}, \tag{7}$$

the transparent carrier density n_{gi}, a dispersion coefficient b and an angular frequency ω_o at the gain peak.

The term B is the self saturation coefficient given by [23], [24]

$$B = \frac{9}{4} \frac{\hbar \omega_p}{\varepsilon_o n_r^2} \left(\frac{\tau_{in}}{\hbar} \right)^2 \sum_i R_{cv}^2 \frac{a_i \xi_i^2 (n_i - n_{gi})}{V_i} \tag{8}$$

where, R_{cv}^2 is the square value of the dipole moment, τ_{in} is the intraband relaxation time and V_i is the effective volume of the i region. D_{pq} is the cross saturation coefficient of mode p caused by mode q and is given with the self saturation coefficient B and the asymmetric saturation coefficient H_{pq} as [24]

$$D_{pq} = \frac{4}{3} \frac{B}{\{(\omega_p - \omega_q)^2 \tau_{in}^2 + 1\}} + \frac{1}{2} H_{pq} \tag{9}$$

$$H_{pq} = \frac{3}{2} \sum_i \frac{(a_i \xi_i)^2 (n_i - n_{gi})}{V_i} \times \left\{ \frac{1}{\tau_s} + \frac{3}{2} \frac{\sum_i a_i \xi_i}{\sum_i V_i} S + \alpha(\omega_p - \omega_q) \right\} \div \left\{ (\omega_p - \omega_q)^2 + \left(\frac{1}{\tau_s} + \frac{3}{2} \frac{\sum_i a_i \xi_i}{\sum_i V_i} S \right)^2 \right\}. \tag{10}$$

G_{th} is the threshold gain level determined by both the loss coefficient κ in the laser and the mirror loss as,

$$G_{th} = \frac{c}{n_r} \left(\kappa + \frac{1}{2L} \ln \frac{1}{R_f R_b} \right) \tag{11}$$

C_{pi} gives a coefficient to include the spontaneous emission to the mode p in the i region

$$C_{pi} = \frac{M_{eq}}{M_{cout}} \frac{a_i \xi_i n_i}{\{[2(\omega_p - \omega_o)/\delta\omega]^2 + 1\}} \tag{12}$$

where $\delta\omega$ is the half width of the emission profile, M_{eq} is an equivalent total number of the internal cavity modes, which is counted to be the number of existing modes in the spontaneous emission profile as [25], [26]

$$M_{eq} = \delta\omega n_r L / 2c \tag{13}$$

while, M_{count} is total number of the internal cavity modes counted really in the calculation. The ratio M_{eq}/M_{cout} is introduced to count total amount of spontaneous emission by all lasing modes, which leads to more accurate calculation of the quantum noise especially at operation with a lower injection current [25], [26].

The factor α in Eqs. (3) and (4) is the so called line-enhancement factor which gives the ratio of (refractive index change)/(gain change). $\overline{n_i}$ is the timely averaged carrier density in the i region.

The terms with operation of Re { } in Eq. (3) indicate effect caused by re-injection of the light, where $U_p^{(1)}$ and $U_p^{(2)}$ are coefficients corresponding to the one round trip and the two round trip propagations to the reflecting point, respectively, given by

$$U_p^{(1)} = \sqrt{\eta \Gamma / R_f} (1 - R_f) e^{j[\varphi_p(t-\tau) - \varphi_p(t) - \omega_p \tau]} \tag{14}$$

$$U_p^{(2)} = \sqrt{\eta}\, \Gamma (1 - R_f) e^{j[\varphi_p(t-2\tau) - \varphi_p(t) - 2\omega_p \tau]}. \tag{15}$$

Other higher terms of the round trip are neglected.

The phase delay $\omega_p \tau$ has to be counted for all lasing modes having different values of ω_p, and is characterized only by a phase delay parameter $\omega_o \tau$ in relation of,

$$\omega_p \tau = (\omega_p - \omega_o)\tau + \omega_o \tau \tag{16}$$

Variation of the phase φ_p in Eq. (4) is characterized by a value α of the line enhancement factor. The terms with operation of Im { } in Eq. (4) give the effect caused by the re-injection of the light.

The coefficient $A_{pi} + j\alpha a_i \xi_i (n_i - \overline{n_i})$ in Eqs. (3) and (4) comes from an induced linear polarization by the re-injected light. On the other hand, a coefficient of $c/n_r L$ has been used as a corresponding coupling coefficient by many authors [15]–[22] by counting variation of the effective threshold gain level G_{th} due to the re-injected light as introduced by R. Lang and K. Kobayashi [15]. Our analysis and the previous works may give same evaluations for the re-injection, because our value of $\sqrt{\eta\Gamma}$ as in Eqs. (14) and (15) can replace value of $(1 + j\alpha a_i \xi_i (n_i - \overline{n_i})/A_{pi})\sqrt{\Gamma} \approx (1 + j\alpha)\sqrt{\Gamma}$ in the previous works [16]–[21].

Crosssectional view of a laser structure is shown in Fig. 2. Here, Act. is the active region made of a non-doped direct transition material, Adj. is the adjacent region made of same material of the active region but has no current injection, Cap is the cap region made of a p-type indirect transition material, Cu.Bl. is the current blocking region made of an n-type direct transition material, Cl.1 and Cl.2. are the cladding regions made of a p-type indirect transition material, and Buf.1 and Buf.2 are the buffer regions made of an n-type indirect transition material. Both Adj. and Cu.Bl. regions work as saturable absorbing regions in this model, since they are made of direct transition materials with small band gaps.

Table 1 Assumed material parameters.

No	Name	Type	x	w_i [m]	d_i [m]	τ_{si} [sec]	a_i [m^3/sec]	n_{gi} [m^{-3}]	
6	Electr.	Metal							
3	Cap	p	0.50	3.0×10^{-6}	2.0×10^{-6}	1.0×10^{-5}	0.0	0.0	
4	Cu.Bl.	n	0.0	Calcu.	2.0×10^{-6}	1.5×10^{-9}	2.50×10^{-11}	2.50×10^{25}	
7	Cl.1	p	0.50	3.0×10^{-6}	3.0×10^{-7}	1.0×10^{-5}	0.0	0.0	
5	Cl.2	p	0.50	Calcu.	3.0×10^{-7}	1.0×10^{-5}	0.0	0.0	
1	Act.	i	0.15	3.0×10^{-6}	8.0×10^{-8}	Calcu.	2.76×10^{-12}	1.20×10^{24}	
2	Adj.	i	0.15	Calcu.	8.0×10^{-8}	Calcu.	2.50×10^{-11} 2.76×10^{-12}	2.50×10^{24} 1.20×10^{24}	for $n_2 < 2.50\times10^{24}$ for $n_2 \geq 2.50\times10^{24}$
9	Buf.1	n	0.50	3.0×10^{-6}	2.0×10^{-5}	1.0×10^{-5}	0.0	0.0	
10	Buf.2	n	0.50	Calcu.	2.0×10^{-5}	1.0×10^{-5}	0.0	0.0	

Equation (5) characterizes variation of the carrier density n_i in the i region. The summed terms multiplied with the linear gain coefficient A_{pi} indicate that the effective photon number of mode p under the optical feedback becomes $|\sqrt{S_p(t)} + U_p^{(1)}\sqrt{S_p(t-\tau)} + U_p^{(2)}\sqrt{S_p(t-2\tau)}|^2$. τ_{si} is the carrier life time, which is given with constant values in both the indirect transition material and the doped materials. However, τ_{si} is given with a calculated value in terms of a proportional constant A_s as,

$$\tau_{si} = 1/(A_s n_i) \tag{17}$$

for the case of the non-doped direct transition material. T_{ij} is an equivalent carrier lifetime characterizing carrier diffusion from i to j regions and is determined by the stripe width W_i, the diffusion constant D_c and a factor f_{ij} $(0 \leqq f_{ij} \leqq 1)$ as [10], [26]

$$T_{ij} = W_i^2/(2D_c\, f_{ij}) \quad \text{or} \quad T_{ij} = d_i^2/(2D_c\, f_{ij}) \tag{18}$$

for diffusion from an internal to an external regions, or as

$$T_{ji} = V_j T_{ij} f_{ij}/(V_i\, f_{ji}) \tag{19}$$

from an external to an internal region. V_i is an effective volume of a region given with the width W_i, the thickness d_i and the cavity length L as

$$V_i = W_i d_i L \tag{20}$$

where, the width in the external region is counted with a smaller value lied between the carrier diffusion length and the spreading range of the optical field [10], [26].

I_{ij} gives the carrier (electron or hole) injection from i to j regions and is represented by injection mechanism k_{ij} and k_{ji} as [26]

$$I_{ij} \equiv k_{ij} - k_{jj} \tag{21}$$

Direction of the carrier injection I_{ij} is same as that of the injection current I for the hole injection, but is inverse for the electron injection.

Besides the principle injected current I_o to the active region, a diffusion current I_d caused by the optical absorption in the Cu.Bl. region is assumed in this paper. The total injection current I is then given as

$$I = I_o + I_d. \tag{22}$$

More detailed discussion on the diffusion current and the leak current are given in Ref. [26].

The total photon number $S(t)$ is given by

$$S(t) = \sum_p S_p(t) \tag{23}$$

and the output power P_{out} is decided by

$$P_{out} = \frac{(1-R_f)\pi c^2 \hbar}{n_r \lambda_o L}\,\overline{S} \times \frac{\ln(1/R_f R_b)}{(1+\sqrt{R_f/R_b})(1-\sqrt{R_f R_b})} \tag{24}$$

where, λ_o $(= 2\pi c/\omega_o)$ is the center wavelength and $\bar{}$ indicates to take the timely averaged value.

2.2 Calculated Example of Pulsation

As calculated numerical examples, the Al_xGa_{1-x} As system is assumed. The assumed material parameters of each region are listed in Table 1. Other parameters are $\lambda_o = 8.267\times10^{-7}$ m, $b = 4.16\times10^{-4}$ sec^{2}m^{-3}, $\delta\omega = 7.00\times10^{13}$sec^{-1}, $n_r = 3.60$, $\kappa = 1000\,\mathrm{m}^{-1}$, $R_b = 0.60$, $R_f = 0.30$, $L = 3.00\times10^{-4}$ m, $A_s = 1.16\times10^{-16}$ m^{3}sec^{-1}, $9\omega_o\tau_{in}^2 R_{cv}^2/(4\varepsilon_o n_r^2\hbar) = 1.40\times10^{-23}$ m^3, $D_c = 3.6\times10^{-3}$ m^{2}sec^{-1}, $\alpha = 2.7$ and $M_{count} = 11$.

The factors describing the ambipolar diffusion between the Act.(1) and the Adj.(2) regions are

$$f_{12} = f_{21} = 1.0. \tag{25}$$

The Cu.Bl. (4) regions work as the saturable absorbing regions in this model. The holes generated by the optical absorption in the Cu.Bl. region will diffuse into the Cl.2 (5) regions because the potential of the valence band in the Cl.2 region is much lower than that in the Cu.Bl. region. We take into account this diffusion effect by putting

$$f_{45} = 0.05 \quad \text{and} \quad f_{54} = 0. \tag{26}$$

All other factors of f_{ij} are put to be zero. That is, all equivalent carrier life times T_{ij} and T_{ji} are put infinite except T_{12}, T_{21} and T_{45}.

The hole diffusion from the Cu.Bl. to the Cl.2 regions has to induce hole injection I_d from the p-side electrode to the Cu.Bl. region to keep the electrical neutral condition

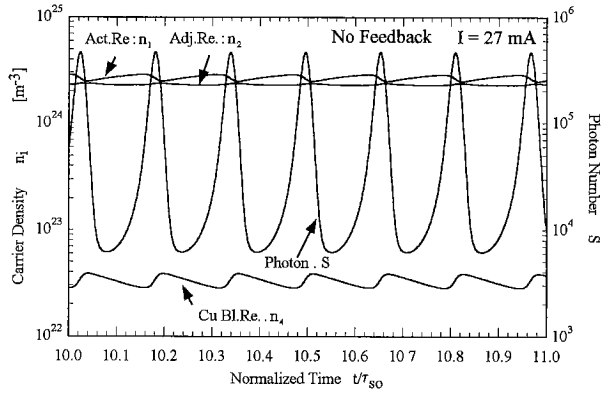

Fig. 3 A calculated example of pulsation shapes without optical feedback. Variation of the carrier densities in the Adj. and the Cu.Bl. regions are out of phase to that in the Act. region.

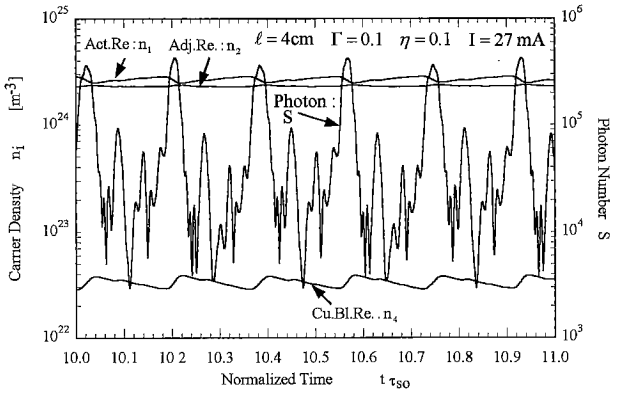

Fig. 4 A calculated example of pulsation shapes with optical feedback. The pulsating operation is disturbed by the optical feedback.

$$I_d = k_{45} = en_4V_4/T_{45} \ . \tag{27}$$

The holes diffused into the Cl.2 regions will flow along the Cl.2 regions and recombine with electrons in the same layer with the Act. and the Adj. regions but at far places from these regions.

As a result, the current components are interrelated to the total injection current I and the diffusion current of Eq. (27) through

$$I_{63} = I_{31} = I_o = I - I_d \tag{28}$$

$$I_{64} = I_{56} = I_d \tag{29}$$

where, I_{56} corresponds to the current flow from the Cl.2 (5) region to the n-side electrode (6') through recombination at far positions to the Adj. region.

The pulsing operation is examined by performing the numerical integration of Eqs. (3) to (5) using the coefficients discussed in earlier. Since the field distribution function $\Phi_p(\mathbf{r})$ varies with the carrier densities, the distribution is re-calculated in each time step following the manner given in Ref. [26].

Calculated examples of the pulsing operation are shown in Fig. 3 for operation without optical feedback ($\Gamma = 0$) and operation with optical feedback in Fig. 4, where $\tau_{so} = 5 \times 10^{-9}$ sec $= 5$ nsec is a time constant giving normalization in the calculation. The time varying step in the calculation is $\tau_{so}/1000 = 5$ psec.

Time variation of the carrier densities in the Adj. and the Cu.Bl. regions are out of phase with that in the Act. region, indicating that both the Adj. and the Cu.Bl. regions work as the saturable absorbing regions in this model. The photon number S reveals a peak when the carrier density n_1 in the Act. is reducing and n_2 in the Adj. and n_4 in the Cu.Bl. are increasing. The pulsing operation is disturbed by the optical feedback as shown in Fig. 4, whose spectrum profile for the photon number is given in Fig. 5.

More detailed investigation on the pulsing operation with variations of the injection current I, the feedback ratio Γ and the distance ℓ will be shown with the noise characteristics in the following section.

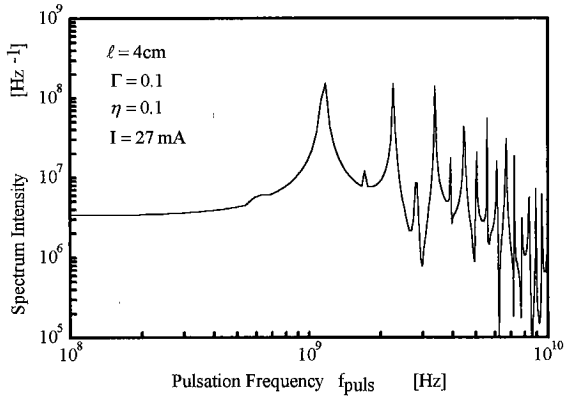

Fig. 5 The Spectrum Profile of the Pulsed Output with Optical Feedback.

3. Noise Calculation

3.1 Equation for Noise Calculation

The basic Eqs. (3) to (5) have been obtained by introducing the optical feedback as terms characterized by the time delay τ. Direct calculation of the feedback noise might be possible by adding the noise sources to these equations in forms of random number generators and by performing time integration. However, this direct calculation may require terrible calculation processes to fix both the amplitudes and the correlations among the noise sources.

The alternative approach to calculate the noise is to apply the mode competition treatment in which the amplitudes and the mutual correlations among the noise sources are well defined [4], [6]–[9]. Both the internal cavity mode and the external cavity mode, built by the laser facet and the reflecting point, should be taken into account as existing modes under the optical feedback [5], [6].

Equation (3) is rewritten as a dynamic equation

including the noise source $F_p(t)$ as,

$$\frac{dS_p}{dt} = \left\{ \sum_i A_{pi} - BS_p - \sum_{q \neq p} D_{pq} S_q - G_{thp} \right\} S_p + \sum_i C_{pi} + F_p(t) \tag{30}$$

where, the mode number p is applied to both the internal and external cavity modes in this section. The threshold gain level G_{thp} is not identical for different lasing modes anymore because of the interference between the internal and external cavities.

Variation of the carrier density n_i in Eq. (5) is rewritten as variation of the carrier number $n_i V_i$, because the noise is originated from fluctuations on any quantum number not on its spatial density. Another noise source $Q_i(t)$ is also added to this equation, so that

$$\frac{dn_i V_i}{dt} = -\sum_p A_{pi} S_p - \frac{n_i V_i}{\tau_{si}} + \sum_{j \neq i} \left(-\frac{n_i V_i}{T_{ij}} + \frac{n_j V_j}{T_{ji}} + \frac{I_{ji} - I_{ij}}{e} \right) + Q_i(t) \,. \tag{31}$$

The noise source terms can be expanded into angular frequency components as

$$F_p(t) = \int F_{p\Omega} e^{j\Omega t} d\Omega \tag{32}$$

$$Q_i(t) = \int Q_{i\Omega} e^{j\Omega t} d\Omega \tag{33}$$

Then the injection current, the carrier density and the photon number are also rewritten as

$$I_{ij} = \overline{I_{ij}} + \Delta I_{ij}(t) + \int I_{ij\Omega} e^{j\Omega t} d\Omega \tag{34}$$

$$n_i = \overline{n_i} + \Delta n_i(t) + \int n_{i\Omega} e^{j\Omega t} d\Omega \tag{35}$$

$$S_p = \overline{S_p} + \Delta S_p(t) + \int S_{p\Omega} e^{j\Omega t} d\Omega \tag{36}$$

where, $\bar{}$ indicates timely averaged values while terms with Δ are timely varying components due to the pulsing operation.

The following equations are obtained by processes of substituting Eqs. (32)–(36) into Eqs. (30) and (31), multiplying $e^{-j\Omega t}$ both side of the obtained equations, and finally taking the time average. The correlations between the pulsing components and the fluctuated terms are ignored. The obtained equations are,

$$\left(j\Omega + \frac{K_p}{\overline{S_p}} + \overline{BS_p} \right) S_{p\Omega} + \sum_{q \neq p} \overline{D_{pq} S_p} \, S_{q\Omega} - \sum_i \overline{\frac{1}{V_i} \left(a_i \xi_i S_p + \frac{C_{pi}}{n_i} \right)} \overline{V_i} \, n_{i\Omega} = F_{p\Omega} \tag{37}$$

$$\sum_p \overline{A_{pi}} \, S_{p\Omega} + \left[-j\Omega + \overline{\frac{a_i \xi_i}{V_i}} \sum_p S_p + \overline{\left(\frac{1}{\tau_{si}} \right)} + \sum_{j \neq i} \overline{\left(\frac{1}{T_{ij}} \right)} \right] \times \overline{V_i} \, n_{i\Omega} - \sum_{j \neq i} \overline{\left(\frac{1}{T_{ji}} \right)} \overline{V_j} \, n_{j\Omega} + \sum_{j \neq i} \frac{I_{ji\Omega} - I_{ij\Omega}}{e} = Q_{i\Omega} \tag{38}$$

where

$$K_p \equiv \left(\overline{G_{thp}} + \sum_{q \neq p} \overline{D_{pq} S_q} + \overline{BS_p} - \sum_i \overline{A_{pi}} \right) \overline{S_p} = \sum_i \left\{ \overline{C_{pi}} + \overline{a_i \xi_i \Delta n_i \Delta S_p} \right\} \tag{39}$$

The defined term K_p is very important to determine the effect of noise reduction with the help of the self-sustained pulsation as will be discussed later.

The carrier injection component $I_{ij\Omega}$ is zero when I_{ij} is taken as the injection current I from the constant current source, and is characterized with $n_{i\Omega}$ and $n_{j\Omega}$ when I_{ij} is the diffusion current I_d. Then the fluctuated terms $S_{p\Omega}$ and $n_{i\Omega}$ in Eqs. (37) and (38) can be expressed as functions of the variables $F_{p\Omega}$ and $Q_{i\Omega}$.

Magnitudes of the noise sources are determined by the DC values as [26]–[28]

$$\langle F_{p\Omega} \, F_{q\Omega} \rangle = \int F(t) F(t+\tau) e^{j\Omega\tau} d\tau = 2 \sum_i \left(\overline{A_{pi} S_p} + \overline{C_{pi}} \right) \delta_{p,q} \tag{40}$$

$$\langle Q_{i\Omega}^2 \rangle = 2 \left\{ \sum_p \overline{A_{pi} S_p} + \overline{\frac{n_i V_i}{\tau_{si}}} + \sum_{j \neq i} \left[\overline{\left(\frac{n_i V_i}{T_{ij}} \right)} + \frac{\overline{k_{ji}} + \overline{k_{ij}}}{e} \right] \right\} \tag{41}$$

$$\langle F_{p\Omega} \, Q_{i\Omega} \rangle = -(\overline{A_{pi} S_p} + \overline{C_{pi}} + \overline{a_i \xi_i n_{gi} S_p}) \tag{42}$$

$$\langle Q_{i\Omega} \, Q_{j\Omega} \rangle = -\left[\overline{\left(\frac{n_i V_i}{T_{ij}} \right)} + \overline{\left(\frac{n_j V_j}{T_{ji}} \right)} + 2 \frac{\overline{k_{ji}} + \overline{k_{ij}}}{e} \right] \tag{43}$$

where, k_{ij} is given by the detailed mechanism forming the carrier injection I_{ij} as introduced in Eq. (21) [26].

Finally, the relative intensity noise (RIN) is defined using the fluctuated value and the timely averaged value of the photon as

$$RIN = \frac{\left\langle \left| \sum_p S_{p\Omega} \right|^2 \right\rangle}{\left(\sum_p \overline{S_p} \right)^2} \tag{44}$$

3.2 Internal Cavity Mode Competition

The timely averaged values in Eqs. (37)–(44) are evaluated through calculation of the pulsing operation in Sect. 2. By regarding all counted modes, $M_{count} = 11$ in the example, as internal cavity modes with an angular frequency separation of

$$\omega_{p+1} - \omega_p = \pi c/n_r L, \tag{45}$$

and the threshold gain level G_{thp} of mode p as that of the laser cavity itself,

$$G_{thp} = G_{th} \tag{46}$$

the RIN is evaluated as the mode competition noise raised by the internal cavity modes. The increasing effect of the quantum noise coming from the carrier transportation among separated regions discussed in Ref. [26] is also included in the investigated noise level.

3.3 External Cavity Mode Competition

By applying the mode number p to all the external cavity modes, the RIN due to the external mode competition could be calculated. However, exact determination of each external cavity mode is difficult, because the resonance and the cut off conditions vary instantaneously with variation of the carrier density n_i through variation of the refractive index n_r under the pulsing operation.

We solve this problem with an approximated treatment of the two mode competition [4], [8]. Even though the lasing modes themselves shift and jump during the pulsing operation, the lasing operation is held by several modes successively. These lasing modes consist with groups of adjoining external modes distributed over the internal cavity modes. We pick up two modes successively in each group and assign a number μ for the sorter wavelength side mode and a number ν for the longer wavelength side mode. Then we define the photon number S_p and S_q as summed values of S_μ and S_ν, respectively, over the all internal cavity modes, such that

$$S_p = \sum_\mu S_\mu \quad \text{and} \quad S_q = \sum_\nu S_\nu \,. \tag{47}$$

Such approximated treatment seems effective because difference between the optical frequencies of the adjoining two modes is a principal parameter to determine the mode competition noise. This optical frequency difference is commonly defined over the internal modes by

$$\omega_\mu - \omega_\nu = \omega_p - \omega_q = \pi c/\ell \,. \tag{48}$$

Effectiveness of this approximated treatment is confirmed by comparing the calculated results with the experimentally measured data as shown later.

Here we determine a condition to build up the multi external modes. We put the phase change of a mode μ for the one round trip in the external cavity as

$$\theta_\mu \equiv 2\ell\omega_\mu/c \tag{49}$$

The resonance condition of the mode μ over both the internal cavity and the external cavity is given by [6], [8]

$$\frac{n_r L}{\ell}\theta_\mu + (1 - R_f)\sqrt{\frac{\eta\Gamma}{R_f}}\sin\theta_\mu = 2k\pi \tag{50}$$

where, k is a number for the internal cavity modes. When the feedback ratio Γ is small enough, the mode μ is non the less the internal cavity mode k.

By increasing the feedback ratio Γ, Eq. (50) goes to take multi solutions for μ. We assign another solution for a number ν. Then the following equation is obtained from Eq. (50) as the condition of building up the external cavity mode,

$$\frac{n_r L}{\ell}(\theta_\mu - \theta_\nu) = -2(1 - R_f)\sqrt{\frac{\eta\Gamma}{R_f}}\cos\frac{\theta_\mu + \theta_\nu}{2}\sin\frac{\theta_\mu - \theta_\nu}{2} \tag{51}$$

We assume that the mode ν locates at longer wavelength side than the mode μ, $\omega_\mu > \omega_\nu$. The minimum value of the feedback ratio Γ is obtained when $\theta_\mu - \theta_\nu = \pi$, because the summed value of the two phases $\theta_\mu + \theta_\nu$ has a very large value and the condition of $\cos[(\theta_\mu + \theta_\nu)/2] = -1$ is easily obtained by adjusting the distance ℓ within the wavelength λ_o. Then the condition for build up of the external mode becomes

$$\Gamma \geqq \Gamma_c = \frac{R_f}{\eta}\left\{\frac{\pi n_r L}{2\ell(1 - R_f)}\right\}^2 \tag{52}$$

where Γ_c is called the critical feedback ratio [6]. This equation is a corrected one to Eq. (17) in our previous publication of Ref. [6]. This result is obtained from the resonance condition in a double cavity as given in Eq. (50) without introduction of dynamic variation of the carrier density. Our result also corresponds to the previously obtained results started with the coupling coefficient of $c/n_r L$ [16]–[20], whose obtained feedback ratios are values multiplied by a factor $\eta/\sqrt{1+\alpha^2}$ to our result in Eq. (52).

The frequency separation $\omega_\mu - \omega_\nu$ increases with the feedback ratio from $\pi c/2\ell$ and approaches immediately to the value $\pi c/\ell$ in Eq. (48). Then we substitute the value in Eq. (48) in the numerical calculation.

The fluctuations of the carrier densities $n_{i\Omega}$ are treated as a combined value of the carrier number N_Ω in this noise calculation for simple treatment. The increasing effect on the quantum noise [26] due to carrier transportation among separated regions has been counted in the calculation of the internal cavity mode competition in the last subsection and may not be necessary in this subsection. We define Ω components for summed values of the carrier and the noise sources over

all regions as

$$\sum_i \overline{V_i} n_{i\Omega} \equiv N_\Omega \tag{53}$$

$$\sum_i Q_{i\Omega} \equiv Q_\Omega \,. \tag{54}$$

By summing up Eq. (38) over all regions, we get the following simple equations for the external mode competition,

$$\left(j\Omega + \frac{K_p}{\overline{S_p}} + \overline{BS_p}\right) S_{p\Omega} + \overline{D_{pq}S_p}\, S_{q\Omega} - \sum_i \overline{\frac{a_i\xi_i}{V_i}\left(S_p + \frac{M_{eq}}{2}\right)} N_\Omega = F_{p\Omega} \tag{55}$$

$$\sum_i \overline{A_{pi}}\, S_{p\Omega} + \sum_i \overline{A_{qi}}\, S_{q\Omega} + \left[-j\Omega + \sum_i \overline{\frac{a_i\xi_i}{V_i}(S_p + S_q)} + \sum_i \overline{\left(\frac{1}{\tau_{si}}\right)}\right] N_\Omega = Q_\Omega \tag{56}$$

$$\langle Q_\Omega^2 \rangle = 2\sum_i \left\{\overline{A_{pi}(S_p + S_q)} + \overline{\frac{n_i V_i}{\tau_{si}}}\right\} \tag{57}$$

$$\langle F_{p\Omega} Q_\Omega \rangle = -\sum_i \left(\overline{A_{pi}S_p} + \frac{M_{eq}}{2}\overline{a_i\xi_i n_i} + \overline{a_i\xi_i n_{gi} S_p}\right) \tag{58}$$

where, $M_{count} = 2$ is used to represent inclusion of the spontaneous emission from all internal modes M_{eq} to the two modes. The relation of $A_{qi} = A_{pi}$ is applied in case of the external cavity mode competition, because the dispersion term $b(\omega_p - \omega_q)^2$ in Eq. (6) is negligible. Another equation for $F_{q\Omega}$ is obtained by changing p and q in Eq. (55).

Evaluation of the introduced term K_p in Eq. (39) is important for the noise calculation but is not easy, because the threshold gain level G_{thp} changes in a complicated manner with the carrier density n_i through variation of the refractive index n_r. We treat this problem in the following basing on the equivalent two mode competition treatment.

Since we assumed only two modes p and q, the total photon number is given as summed value of these modes as

$$S = S_p + S_q \tag{59}$$

We also assume that the variation ratio of the photon numbers due to the self-sustained pulsation is equal for these modes,

$$\frac{\Delta S}{\overline{S}} = \frac{\Delta S_p}{\overline{S_p}} = \frac{\Delta S_q}{\overline{S_q}} \tag{60}$$

and we introduce a parameter m called the effective modulation index as

$$m = \sum_i \overline{a_i\xi_i \Delta n_i \Delta S} \Big/ \sum_i \overline{a_i\xi_i n_i}\ \overline{S} \tag{61}$$

Then the term K_p in Eq. (39) is given by the DC terms and the modulation index m as

$$K_p = \sum_i \{\overline{C_{pi}} + \overline{a_i\xi_i \Delta n_i \Delta S_p}\} = \sum_i \overline{a_i\xi_i n_i}(M_{eq}/2 + m\overline{S_p}) \tag{62}$$

The modulation index m varies with not only the pulsation amplitudes of the carrier densities Δn_i and the photon number ΔS but also with the phase difference of the variation phase between Δn_i and ΔS. Since the phase difference is around $\pm\pi/2$ as found in Figs. 3 and 4, the modulation index m sensitively changes with the laser structure and the operating conditions.

From Eq. (39), the difference between the timely averaged threshold gain levels of modes p and q becomes

$$\overline{G_{thq}} - \overline{G_{thp}} = (\overline{B} - \overline{D_{qp}})\overline{S_p} + (\overline{D_{pq}} - \overline{B})\overline{S_q} - \sum_i \overline{a_i\xi_i n_i}\frac{M_{eq}}{2}\left(\frac{1}{\overline{S_p}} - \frac{1}{\overline{S_q}}\right) \tag{63}$$

The power distribution ratios of the total photon number to $\overline{S_p}$ and $\overline{S_q}$ in Eq. (59) are examined by a condition of getting a local minimum value of the threshold difference $\overline{G_{thq}} - \overline{G_{thp}}$ in the range of $\overline{G_{thq}} - \overline{G_{thp}} \geqq 0$, because the modes p and q should be the most dominant two modes.

Since the modulation index m and the timely averaged terms, such as $\overline{S}$, $\overline{a_i\xi_i n_i}$, $\overline{B}$, $\overline{D_{qp}}$ $\overline{D_{pq}}$, are examined through the pulsing calculation in Sect. 2, the timely averaged photon numbers $\overline{S_p}$ and $\overline{S_q}$ are obtained by Eq. (63). Then noise due to the external mode competition is calculated by Eqs. (55) to (58) together with Eqs. (40) and (44).

Here, the mutual saturation coefficients D_{pq} and D_{qp} in Eqs. (55) and (63) should be substituted with the relation

$$D_{pq} = 2B + H_{pq} \tag{64}$$

together with Eqs. (10) and (48) to be applied for the external modes instead of Eq. (9) because the longitudinal field distribution is identical for both modes p and q in the laser [4], [6] Since we assumed that the mode q locates longer wavelength side of the mode p, sings of these coefficients are $D_{pq} > 0$ and $D_{qp} < 0$.

3.4 Calculated Example of Noise

Our calculating manner of the noise is as follows:

1. The geometrical and the material parameters in Fig. 2 as well as the operating conditions of the injection current I, the feedback distance ℓ and the feedback ratio Γ are set.
2. The pulsing operation is examined by performing

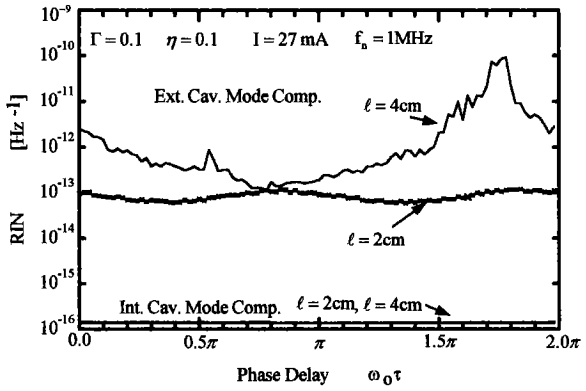

Fig. 6 Variation of the noise with the phase delay. The noise level due to the external mode competition varies sensitively with the phase delay $\omega_o\tau$.

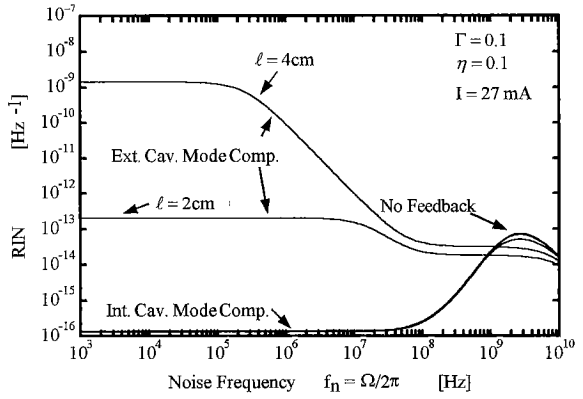

Fig. 7 Frequency spectrum of the noise. Noise increases in the low frequency region due to the external mode competition.

the time integration in Sect. 2 over longer times than $t/\tau_{so} = 13$. The several timely averaged values introduced in Sect. 3 with notation $\bar{}$ are calculated though this pulsing examination.

3. The noise due to the internal cavity mode competition is evaluated using the equations in Sect. 3.2.

4. The noise due to the external cavity mode competition is evaluated applying the equations in Sect. 3.3.

The noise without optical feedback is also examined following items 1 to 3 in the above mentioned manner by putting $\Gamma = 0$. This is almost equivalent to the calculation of the quantum noise discussed in Ref. [26].

The pulsing operation and the noise level sensitively vary with the initial setting of the phase delay $\omega_o\tau$, which has been introduced in Eqs. (14) to (16), as shown in Fig. 6, where f_n $(= \Omega/2\pi)$ is the noise frequency. The variation of $\omega_o\tau$ implies to tune the distance ℓ with accuracy much shorter than the optical wavelength λ_o. The calculation by processing the items 1 to 4 is repeated by changing $\omega_o\tau$ in a range from 0 to 2π with a fine step value. The variation step of $\omega_o\tau$ in Fig. 6 is 0.02π. Calculation of this figure took almost four hours with a conventional work station, because calculation of the pulsing operation is performed with re-examination of the transverse field distribution $\Phi_p(\mathbf{r})$ at each time step of $\tau_{so}/1000$ over a time range longer than $t/\tau_{so} = 13$. Other data represened in Figs. 8 (a) to 10 were calculated with a variation step of $\omega_o\tau$ of 0.21π. The used values of $\omega_o\tau$ in Figs. 7 to 10 except Fig. 8 (a) are found to give the highest noise for each given operating condition. A series of calculations on varying one operating parameter such as I in Fig. 8 required more than ten hours as the computer work.

The frequency spectrum of the noise is shown in Fig. 7, corresponding to operations giving the highest noise in Fig. 6. The noise due to the external cavity mode competition increases in the low frequency range for $\ell = 4$ cm but is rather suppressed for $\ell = 2$ cm. The noise due to the internal cavity mode competition is almost in the same level of the quantum noise [26] when the self-sustained pulsation is kept.

Characteristics for variations of the injection current I, the feedback ratio Γ and the feedback distance ℓ are shown in Figs. 8 (a) to 9 (c). Operation without optical feedback is indicated with "No Feedback" in these figures. The threshold current level of this laser is around 16 mA as shown in Fig. 8 (a). Max.Out. and Min.Out in Fig. 8 (a) indicate the variation of the output power for variation of $\omega_o\tau$. The output power is slightly reduced by the optical feedback in this model for most operating conditions. The pulsation is obtained in the range of $20 \leqq I \leqq 44$ mA by the laser itself, as found in Fig. 8 (b), where the vertical axis represents strength of the pulsation as a ratio of the peak of the pulse to the timely averaged power. The pulsation is obtained in the range of $18 \leqq I \leqq 42$ mA under the optical feedback for the case of $\ell = 2$ cm, but continues beyond 60 mA for $\ell = 4$ cm. Variations of the pulsation frequency f_{puls} are shown in Fig. 8 (c) for cases of without optical feedback and feedback with $\ell = 4$ cm. The frequency for without optical feedback is called the free pulsation frequency f_{po} and is drown in the figure with a solid line in the range of $20 \leqq I \leqq 44$ mA. The peak frequencies of the pulsation in the frequency spectrum as in Fig. 5 under optical feedback are drown with isolated marks for the highest four peaks. Horizontal straight lines with multiple values of $c/2\ell$ indicate resonance frequencies of the external cavity mode. When the pulsation frequencies lie on these lines, the lasing operation is characterized as the mode locking effect with a repeating frequency of $c/2\ell$ rather than the self-sustained pulsation. We found by comparing Figs. 8 (b) to (c) that the pulsing operation with $\ell = 4$ cm for $I > 35$ mA is more like the mode locking effect than in the self-sustained pulsation.

Variations of the noise with the injection current I are shown in Fig. 8 (d). The noise without the optical feedback is well suppressed when the self-sustained pulsation is kept in the range of $20 \leqq I \leqq 48$ mA,

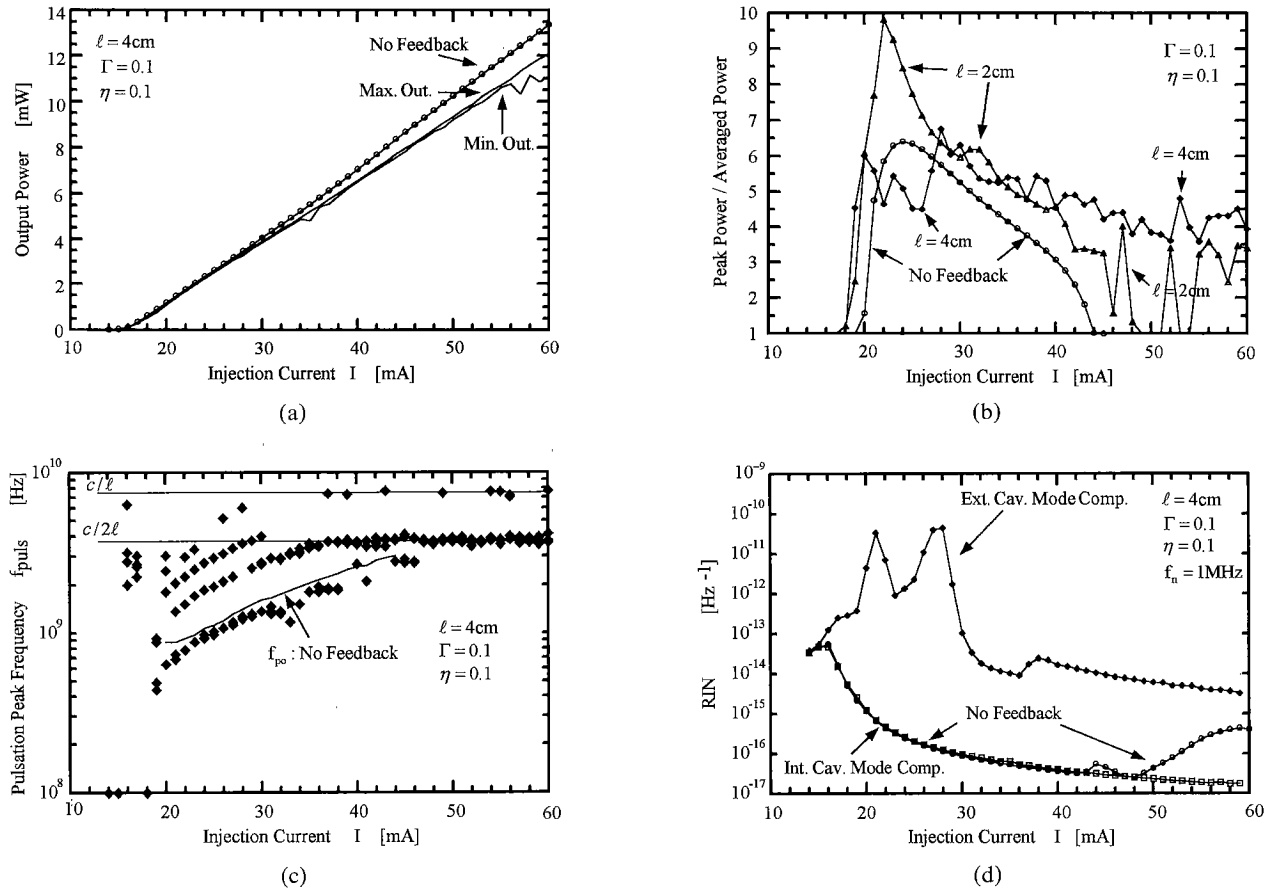

Fig. 8 Characteristics for the current variation. (a) output power, (b) pulsation intensity, (c) pulsation peak frequency, (d) noise.

but increases for $I > 48\,\mathrm{mA}$ due to the mode competition among the internal modes [4]. The noise under the optical feedback is mostly enhanced by the external mode competition. The condition giving the increase of the noise will be understood basing on variation of the free pulsing frequency f_{po} relating to the resonance frequency $c/2\ell$ of the external cavity in the followings.

Figures 9 (a) to (c) plot variation of the characteristics for the reflecting distance ℓ as given by the top horizontal axis. The characteristics are more uniformly represented by the normalized feedback distance $2f_{po}\ell/c$ indicated by the bottom horizontal axis, which is the ratio of the free pulsation frequency f_{po} to the resonance frequency of the external cavity mode $c/2\ell$. Traces of the f_{po} and $c/2\ell$ and their higher harmonics are drown in Fig. 9 (a) with solid lines. The highest four peaks in the pulsation spectrum are plotted as isolated marks. The pulsation frequencies have components fitting to the lines $c/2\ell$ and c/ℓ in the range of $0.5 \leqq 2f_{po}\ell/c \leqq 1.0$. The effective modulation index m defined in Eq. (61) mostly varies centering this range of $0.5 \leqq 2f_{po}\ell/c \leqq 1.0$ as found in Fig. 9 (b). We also observe that the noise in Fig. 9 (c) is enhanced when the effective index m is in the range of $-0.018 \sim -0.016$. The noise is well suppressed in the ranges of $2f_{po}\ell/c \leqq 0.3$ and $2f_{po}\ell/c \geqq 1.2$.

Variation of the noise with the feedback ratio is shown in Fig. 10. The noise due to the external cavity modes starts from the critical feedback ratio given in Eq. (52).

3.5 Comparison with Experimental Measured Data

Characteristics of the experimentally observed noise depend on for structure and material of each device as well as whose operating conditions. However, commercially sold lasers for the compact disk (CD) system and the video disk (CD) system have almost similar structure to that in Fig. 2. Experimentally observed data of Sony SLD131UL are shown in Fig. 11 for variation of the normalized feedback distance. The data fit quantitatively with Fig. 9 (c) whose output power is around $P_{out} = 3\,\mathrm{mW}$. The noise increases in the range of $0.3 < 2f_{po}\ell/c < 1.2$ but has several dips. One different feature between the theoretical calculation and the experimental data is the height of the noise. The data by the theoretical calculation have a higher level than those by experiment. This difference may come from that the phase difference $\omega_o\tau$ was averaged out in the

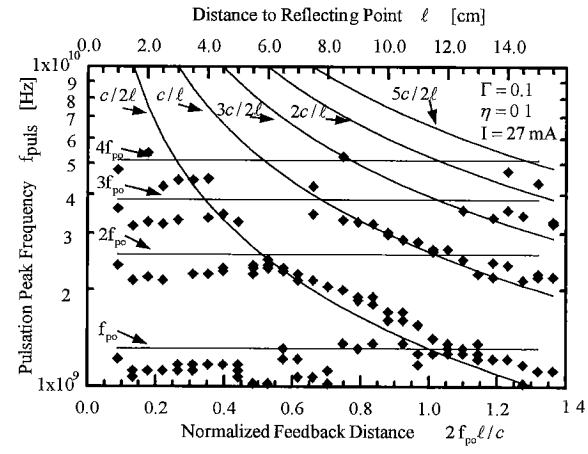

(a)

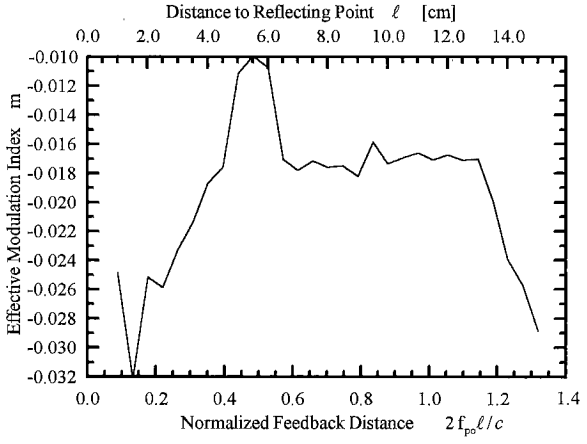

(b)

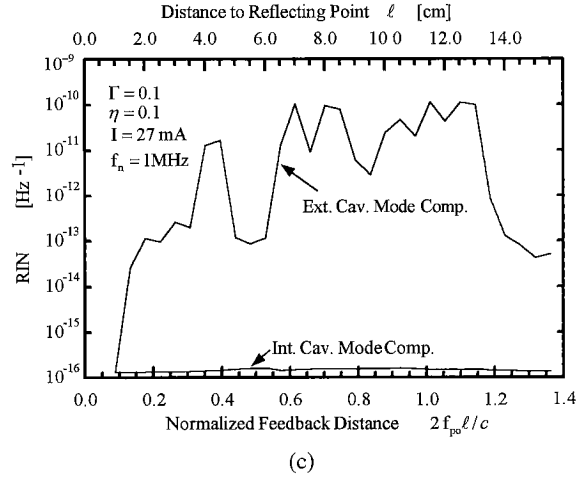

(c)

Fig. 9 Characteristics for the feedback distance. (a) pulsation peak frequency, (b) effective modulation index, (c) noise. Characteristics relating the external mode competition are more uniformly given by using the normalized feedback distance $2f_{po}\ell/c$.

experiment. Reduction more than 10 dB could be expected in the theoretical calculation by averaging the noise with $\omega_o\tau$ as found in Fig. 6. Another difference is

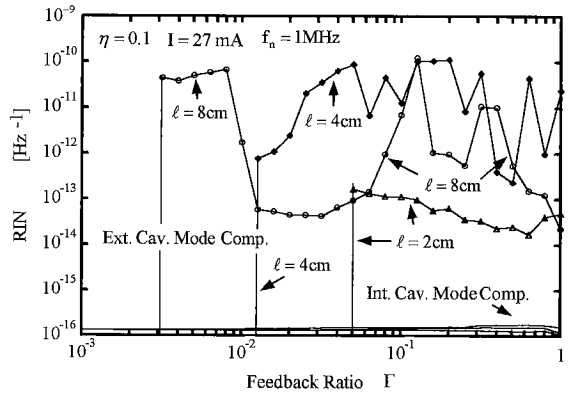

Fig. 10 Variation of the noise with feedback ratio. The external cavity modes start to build up for larger Γ.

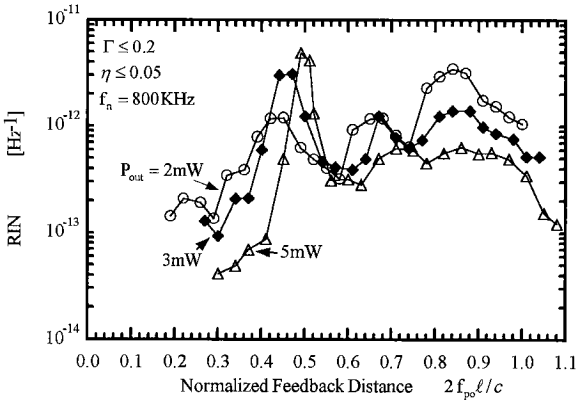

Fig. 11 Experimentally measured noise for variation of feedback distance.

the value of the normalized feedback distance characterizing the profile. The difference may base on insufficient adjustment of the structure parameters in Table 1.

4. Conclusions and Remarks

Lasing characteristics and the generated noise in the self-sustained pulsation lasers under operation with optical feedback were theoretically analyzed with the help of computer simulation. The pulsing operation was analyzed with the timely delayed light injection model, while the noise is evaluated basing on the model for the modes competition phenomena. Theoretically obtained data fit well the experimental data even though the theoretical calculation was approximately done by equivalent treatment of the two mode competition phenomena for the external modes.

The effect of the noise reduction by mean of the self-sustained pulsation or the superposition of the high frequency current is understood to be due to variation of the effective modulation index m defined in Eq. (61) of this paper. Operating states shift with the index, resulting in reduction of the noise under most of the operating conditions but still give an increase of the noise

under several conditions.

The effective modulation index m in the structure given in Fig. 2 of this paper has a negative value as shown in Fig. 9 (b). However, it has positive values in structures having an additional saturable absorbing region parallel to the active region shown in Ref. [26] which is designed to get higher power operation with the self-sustained pulsation for the writing process in the magnet optical disk (MO) system. The operating characteristics and the noise vary with the sign of the modulation index. Theoretical discussion of the variation of the operating conditions with the structure may be the subject of the next work.

Acknowledgement

This research is supported by Sharp Co. Ltd., Sony Co. Ltd., Mitsubishi Electric Co. Ltd. and Fujitsu Lab. Co. Ltd. The author acknowledges Mr. Y. Ishikawa of Kanazawa University for assistance in measuring the noise.

References

[1] A. Oishi, N.Chinone, M. Ojima, and A. Arimoto, "Noise characteristics of high-frequency superposed laser diodes for optical disc systems," Electron Lett., vol.20, pp.821–822, 1984.

[2] S. Matsui, H. Takiguchi, H. Hayashi, S. Yamamoto, S. Yano, and T. Hijikata, "Suppression of feedback-induced noise in short-cavity V-channeled substrate inner stripe lasers with self-oscillation," Appl. Phys. Lett., vol.43, no.3, pp.219–221, 1983.

[3] M. Ohtsu, Y. Otsuka, and Y. Teramachi, "Precise measurements and computer simulations of mode-hopping phenomena in semiconductor lasers," IEEE J. Quantum Electon., vol.QE-19, no.1, pp.108–110, 1985.

[4] M. Yamada, "Theory of mode competition noise in semiconductor injection lasers," IEEE J. Quantum Electron., vol.QE-22, no.7, pp.1052–1059, 1986.

[5] H. Fukui, K. Furuya, and Y. Suematsu, "Suppression of mode hopping noise cased by external reflection in dynamic single mode (DSM) lasers," IEICE Trans., vol.70, no.7, pp.857–864, 1987.

[6] M. Yamada and M. Suhara, "Analysis of excess noise induced by optical feedback in semiconductor lasers based on mode competition theory," IEICE Trans., vol.E73, no.1, pp.77–82, 1990.

[7] M. Yamada and T. Higashi, "Mechanism of the noise reduction method by superposition of high-frequency current for semiconductor injection lasers," IEEE J. Quantum Electron., vol.27, no.3, pp.380–388, 1991.

[8] M. Yamada, "Theoretical analysis of noise-reduction effect in semiconductor lasers with help of self-sustained pulsation phenomena," J. Appl. Phys., vol.79, no.1, pp.61–71, 1996.

[9] M. Yamada, A. Kanamori, and S. Takayama, "Experimental evidence of mode competition phenomena on the feedback induced noise in semiconductor lasers," IEICE Trans. Electron., vol.E79-C, no.12, pp.1766–1768, 1996.

[10] M. Yamada, "A theoretical analysis of self-sustained pulsation phenomena in narrow-stripe semiconductor lasers," IEEE J. Quantum Electron., vol.29, no.5, pp.1330–1336, 1993.

[11] S. Yamashita, A. Ohishi, T. Kajimura, M. Inoue, and Y. Fukui, "Low-noise AlGaAs lasers grown by organometallic vapor phase epitaxy," IEEE J. Quantum Electron., vol.25, no.6, pp.1483–1488, 1989.

[12] T. Takayama, O. Imafuji, M. Yuri, H. Naito, M. Kume, A. Yoshikawa, and K. Itoh, "800 mW peak-power self-sustained pulsation GaAlAs laser diodes," IEEE J. of Selected Topics in Quantum Electron., vol.1, no.2, pp.562–568, 1995.

[13] T. Goto, N. Hayashi, A. Ibaraki, D. Ide, K. Furusawa, K. Yodoshi, and T. Niina, "Low-noise, high-power GaAlAs laser diode with a saturable absorbing layer," MOC'95, Technical Digest, pp.278–281, 1995.

[14] H. Adachi, I. Kidoguchi, T. Fukuhisa, K. Tanaka, M. Amannoh, and A. Takamori, "Reduction of aspect ration in 650-nm band self-sustained-pulsing lasers," Jpn J. Appl. Phys., vol.36, Part 1, no.3B, pp.1876–1879, 1997.

[15] R. Lang and K. Kobayashi, "External optical feedback effect on semiconductor injection laser properties," IEEE J. Quantum Electron., vol.QE-16, no.3, pp.347–455, 1980.

[16] G.P. Agrawal, "Line narrowing in a single-mode injection laser due to external optical feedback," IEEE J. Quantum Electron., vol.QE-20, no.5, pp.468–471, 1984.

[17] B. Tromborg, J.H. Osmundsen, and H. Olsen, "Stability analysis for a semiconductor laser in an external cavity," IEEE J. Quantum Electron., vol.QE-20, no.9, pp.1023–1032, 1984.

[18] G.A. Acket, D. Lenstra, A.J.D. Boef, and B.H. Verbeek, "The influence of feedback intensity on longitudinal mode properties and optical noise in index-guided semiconductor lasers," IEEE J. Quantum Electron., vol.QE-20, no.10, pp.1163–1169, 1984.

[19] C.H. Henry and R.F. Kazarinov, "Instability of semiconductor lasers due to optical feedback from distant reflectors," IEEE J. Quantum Electron., vol.QE-22, no.2, pp.294–301, 1986.

[20] R.W. Tkach and A.R. Chraplyvy, "Regimes of feedback effects in 1.5-μm distributed feedback lasers," IEEE J. Lightwave Technol., vol.LT-4, no.11, pp.1655–1661, 1986.

[21] N. Schunk and K. Petermann, "Numerical analysis of the feedback regimes for a single-mode semiconductor laser with external feedback," IEEE J. Quantum Electron., vol.24, no.7, pp.1242–1247, 1988.

[22] G.H.M. van Tartwijk and M.S. Miguel, "Optical feedback on self-pulsating semiconductor lasers," IEEE J. Quantum Electron., vol.32, no.7, pp.1191–1202, 1996.

[23] M. Yamada, "Transverse and longitudinal mode control in semiconductor injection lasers," IEEE J. Quantum Electron., vol.QE-19, no.9, pp.1365–1380, 1983.

[24] M. Yamada, "Theoretical analysis of nonlinear optical phenomena taking into account the beating vibration of the electron density in semiconductor lasers," J. Appl. Phys., vol.66, no.1, pp.81–89, 1989.

[25] M. Yamada, "Variation of intensity noise and frequency noise with the spontaneous emission factor in semiconductor lasers," IEEE J. Quantum Electron., vol.30, no.7, pp.1511–1519, 1994.

[26] M. Yamada, "A theoretical analysis of quantum noise in semiconductor lasers operating with self-sustained pulsation," IEICE Trans. Electron, vol.E81-C, no.2, pp.290–298, 1998.

[27] H. Haug, "Quantum-mechanical rate equations for semiconductor lasers," Phys., Rev., vol.184, no.2, pp.338–348, 1969.

[28] T.L. Paoli, "Noise characteristics of stripe-geometry double-hetero-structure junction lasers operating

continuously—I. Intensity noise at room temperature," IEEE J. Quantum Electron., vol.QE-11, no.4, pp.276–283, 1975.

Minoru Yamada was born in Yamanashi, on January 26, 1949. He received the B.S. degree in electrical engineering from Kanazawa University, Kanazawa in 1971, and M.S. and Ph.D. degrees in electronics engineering from the Tokyo Institute of Technology, Tokyo in 1973 and 1976, respectively. He joined Kanazawa University in 1976, and is presently a Professor. From 1982 to 1983, he was a Visiting Scientist at Bell Laboratories, Holmdel, NJ, U.S.A. He is currently working in semiconductor injection laser, semiconductor modulator and unidirectional optical amplifier. Dr. Yamada received the Yonezawa Memorial Prize in 1975, the Paper Award in 1976, and the Achievement Award in 1978 from the IECE of Japan.